Scanning probe microscopy explorations on conjugated (macro)molecular architectures for molecular electronics

2002 J. Phys.: Condens. Matter 14 9955

(http://iopscience.iop.org/0953-8984/14/42/309)

INSTITUTE OF PHYSICS PUBLISHING JOURNAL OF PHYSICS: CONDENSED MATTER

J. Phys.: Condens. Matter **14** (2002) 9955–9973 PII: S0953-8984(02)37131-5

Scanning probe microscopy explorations on conjugated (macro)molecular architectures for molecular electronics

Paolo Samorí[1,2] **and Jürgen P Rabe**

Department of Physics—Physics of Macromolecules, Humboldt University Berlin, Invalidenstrasse 110, D-10115 Berlin, Germany

E-mail: samori@frae.bo.cnr.it

Received 17 May 2002
Published 11 October 2002
Online at stacks.iop.org/JPhysCM/14/9955

Abstract

Achieving exquisite control of the structural organization in molecular arrangements of π-conjugated (macro)molecules with tailored chemical functionalities and physical properties is an essential prerequisite for the reproducible fabrication of high-performance molecular electronic devices. This paper reports on the exploitation of scanning probe microscopies to investigate π-conjugated oligomeric and polymeric architectures assembled on flat solid substrates. These techniques provide genuine insight into the structure of the molecular arrangements as well as into their physicochemical properties over a wide range of length scales. Moreover, they allow one to manipulate organic adsorbates with a precision on the molecular scale, opening a pathway towards the nanopatterning of surfaces and the development of single-molecule devices.

(Some figures in this article are in colour only in the electronic version)

1. Introduction

In the last two decades there has been a growing interest in the 'nanoworld', i.e. the science and technology of nanometre-sized objects. The scientific community has been trying to cast new light on the structure of organic, inorganic, and biological materials, probing their chemical and physical properties on a molecular scale, and comparing the properties of a single molecule with those of an ensemble or Avogadro number of molecules. In the framework of the fabrication of molecular electronic devices based on π-conjugated (macro)molecules,

[1] Author to whom any correspondence should be addressed.
[2] New address: Istituto per la Sintesi Organica e la Fotoreattività, CNR Bologna, via Gobetti 101, 40129 Bologna, Italy.

0953-8984/02/429955+19$30.00

one of the major tasks is understanding and controlling the physicochemical properties of the materials over a wide range of length scales. In work in this direction, scanning probe microscopies have played a paramount role, since they allow one to explore organic surfaces on different scale lengths in various ambients [1, 2]. Making use of these techniques it has been possible to approach the nanoworld in various ways which go far beyond pure imaging of a surface: manipulating single molecules at room temperature [3] opening new avenues towards the study of the conformational and nanomechanical properties of individual molecules [2], visualizing Ostwald ripening in polycrystalline structures at the solid–liquid interface [4], stimulating photochemical reactions with light and following the reaction in real-time at interfaces [5, 6], probing the electronic properties of single molecules by means of scanning tunnelling spectroscopy (STS) [7, 8] and inducing with the scanning tunnelling microscope (STM) tip the electroluminescence of a conjugated thin film [9] are just a few examples.

In this paper we discuss the use of scanning probe microscopy techniques to obtain insight into structural and physicochemical properties of single conjugated (macro)molecules and of their molecular architectures as well as to induce conformational transitions in supramolecular objects with a precision on the molecular scale.

2. Scanning probe microscopies

The invention of the STM in 1982 represented a true breakthrough for the nanosciences [10–12]. The STM made it possible for the first time to generate real-space images of surfaces with a resolution on the sub-nanometre scale. The invention of the atomic force microscope (AFM) [13–16] allowed the investigations to be extended to insulating materials such as polymers and biomolecules. A significant advantage of scanning probe microscopies is that they can operate in different media such as air, liquid, and gas streams, expanding in this way the investigations to atmospheres which are technologically more important and also more easily accessible and less expensive than ultrahigh vacuum. As a consequence, they made it possible not only to observe amorphous or crystalline structures of organic adsorbates, but also to follow dynamic phenomena such as chemical reactions [5, 6] as well as the diffusional path of single molecules [4], the healing of a crystalline surface of alkanethiols self-assembled on metallic surfaces [17], and the process of crystallization [18].

Using these techniques, one can in favourable cases achieve a spatial resolution along the X-, Y-, and Z-directions of a fraction of an ångström. The techniques are generally based on a sharp probe (tip) that interacts locally with a sample surface during scanning. The scanning probe microscopes differ as regards the prime physical property that is measured and used to map the surface.

3. Scanning tunnelling microscopy

The STM [10–12] which is the ancestor of this family provides an image of the tunnelling current in a plane across a conductive sample which, in a first crude approximation, corresponds to the topographical map of the sample. More precisely, rather than measuring physical topography, the STM tip probes point by point the probability of tunnelling between tip and surface while scanning. This gives evidence of the electronic local density of states (LDOS) at the surface [19] by sensing the density of filled or unfilled electronic states near the Fermi surface, within an energy range determined by the bias voltage at low voltage [20]. Although great effort has been devoted to the development of theoretical methodologies to supplement experimental results [21–25], more than 20 years on from the STM invention the discrimination between the electronic and the topographic structures of the surfaces under study is still a non-trivial task.

The STM technique is based on the quantum-mechanical effect of electron tunnelling. The tunnelling occurs between two electrodes separated by a gap (or insulating layer) that acts as a potential barrier for the electrons. The tunnelling current decays exponentially with the gap width. The two electrodes are the sample and an atomically sharpened metallic probe; this latter is usually produced by mechanical cutting or chemical etching of a Pt/Ir or W wire [12]. When the tip is brought into close proximity of the sample surface (a few ångströms), applying a bias voltage ($\leqslant$1.5 V) between the two electrodes causes the electrons to tunnel from the sample through the gap into the tip or vice versa, depending upon the sign of the bias voltage [26]. The resulting tunnelling current varies with the tip-to-sample spacing, and it is this signal which is used to create the STM image.

In the STM a sample is scanned in either of two modes: *constant-height mode* or *constant-current mode*. In *constant-height mode*, the tip scans in a horizontal plane above the sample and the tunnelling current changes depending on the topography and the local surface electronic properties of the sample. The tunnelling current measured at each point on the sample surface represents the data set. In *constant-current mode*, the STM uses a feedback loop that enables the tunnelling current to be kept constant by adjusting the height of the scanner at each measurement location. For example, when the system detects an increase in tunnelling current, it adjusts the voltage applied to the piezoelectric scanner in order to enhance the distance between the tip and the sample. In *constant-current mode*, the motion of the scanner constitutes the data set. If the system keeps the tunnelling current constant to within a few per cent, the tip-to-sample distance will typically be constant to within a few hundredths of an ångström. Each mode has advantages and disadvantages.

Constant-height mode is faster because the system does not have to move the scanner up and down, but it provides useful information only for locally smooth surfaces. For this reason it is currently employed to investigate molecular monolayers on atomically flat substrates with a submolecular resolution.

Constant-current mode can measure rougher surfaces with high precision, but the measurement takes more time and the lateral resolution that can be achieved is usually smaller due to the difficulty in achieving a proper setting of the feedback loop which allows the tip to follow the surface roughness and not to introduce a periodic noise in the data set.

The contrast in the images recorded by STM in the *constant-height mode* is mainly determined by the difference between the energies of the molecular states of the adsorbate and the Fermi level of the substrate. For example, for organic molecules adsorbed on graphite, due to a larger energy difference, aliphatic chains generally appear darker than moieties with π-electrons, provided that the moieties are lying equally flat on the substrate [23]. In the case of a given conjugated molecule which is located along the Z-axis at different distances from the surface, the contrast depends additionally on the degree of spatial overlap of the electronic states of the adsorbate with those of the substrate [27]

The biggest limitation of STM is that it cannot image thick insulating layers. Given the possibility of probing currents in the picoampere range, the thickness of a non-conductor layer can be at maximum around 2 nm [28]. Two new modes which have been employed successfully and will be described in the text are the STS mode, which allows one to investigate the electronic properties of single molecules [7, 8], and the tip-induced electroluminescence mode of a conjugated thin film [9].

4. Atomic force microscopy

The invention of AFM [13–16] in 1986 by Binnig and co-workers has overcome the problem of imaging samples with a low electrical conductivity. In fact, with the prime physical property

that is measured with this apparatus being the interaction force between a sharp conical tip and the sample surface, investigations can be performed on electrical conductors as well as semiconductors and organic and even biological materials.

The AFM probes the surface of a sample with a sharp tip, exhibiting a terminal radius often <10 nm. The tip is located at the free end of a ~ 100 μm long cantilever with an elastic modulus which can be as low as tenths of N m^{-1}. Forces of a few piconewtons between the tip and the sample surface cause deflections of the cantilever on the ångström scale. In the commonest scheme, a laser beam bounces off the back of the cantilever onto a position-sensitive photodetector (PSD). As the cantilever bends, the position of the reflected laser beam on the detector shifts. The PSD itself can measure displacements of light beams as small as 1 nm. The ratio of the path length between the cantilever and the detector to the length of the cantilever itself produces a mechanical amplification. As a result, the system can detect sub-ångström vertical movements of the cantilever tip. The measured cantilever deflections enable the computer to generate a map of the surface topography. This apparatus is also called a scanning force microscope (SFM), which is a suitable name in particular when studies are carried out on a scale spanning from the micrometre down to a few nanometres.

In the simplest mode of AFM operation, known as the contact mode, the AFM tip makes soft 'physical contact' with the sample. In analogy to the STM modes introduced previously, the AFM can be employed either in *constant-height mode* or in *constant-force mode*. The major drawback of the contact mode AFM is the presence of strong interaction forces between the tip and the surface, including also frictional forces, which can cause sample deformation. In particular, using very stiff cantilevers it is possible to exert large forces on the sample, opening new ways to manipulate the surface with a precision on the molecular scale. In order to avoid the undesired deformation of the sample, i.e. to decrease the magnitude of the interacting forces between the tip and the surface, alternative modes have been constructed in which the AFM cantilever vibrates near (of the order of 1–10 nm away from) the surface of a sample. In these modes, which can be called dynamic modes, the system detects the shift in the amplitude and the phase of the swing of the cantilever while the tip scans over the sample. The amplitude of the cantilever oscillation is kept constant with the aid of a feedback system that moves the scanner up and down. With the amplitude kept constant, the system is expected to also maintain the average tip-to-sample distance constant. The sensitivity of this detection scheme provides sub-ångström vertical resolution in the image, as in contact mode AFM. Due to the elimination of the shear forces that are acting between the tip and sample, these modes are particularly suitable for studying soft materials such as organic and even biological films. Also, as a consequence of the reduction of the overall interaction forces between the tip and the sample surface, these modes do not suffer from tip or sample degradation effects. The dynamic modes which are commonly used differ essentially with regard to the distance of the tip from the surface during the vibration. While in the *non-contact mode* the tip oscillates far from the surface, in *Tapping Mode*™ (TM-AFM), known also as intermittent-contact AFM, the vibrating cantilever tip is brought closer to the sample in such a way that at the bottom of its travel it just barely hits, or 'taps' the sample [15, 29, 30]. More recently, another version of the Tapping Mode has been developed which has been termed phase imaging: it detects the variation in the phase of the vibrations upon interaction with a surface. This allowed further increase in the spatial resolution [31–33]. The contrast in this imaging mode is particularly sensitive to differences in surface adhesion and viscoelasticity; it is therefore an appropriate tool for the detection of different phases of materials coating the sample surface. Unfortunately, the spatial resolution in the X–Y plane which can be achieved with the dynamic modes is only of a few nanometres, which is lower than that of the contact mode [16]. In fact the relevant forces in the Tapping Mode are more long range, including van der Waals attractions between the tip

and the sample. In contrast, the contact mode is well described with short-range repulsions, which are more strongly distance dependent.

5. Thin-film preparation and SPM visualization

The self-assembly of highly ordered molecular nanostructures is governed by the interplay of *intra*molecular as well as *inter*molecular and interfacial interactions. The control of the growth of hybrid organic–inorganic architectures towards well-defined structures with desired organization requires a proper choice of the molecular structures of the components, including the solid substrate, as well as a proper design of the processing. Today's capability to follow and to control the process of the self-assembly benefited tremendously from the advent of scanning probe microscopy techniques which have been exploited thoroughly in the exploration of a large number of conjugated (macro)molecules at surfaces and interfaces. These investigations have been carried out in different environments and under different operating conditions. One ambient, which is very suitable also for a variety of other surface science investigation methods, is ultrahigh vacuum, which offers the advantage of being fully controlled and clean. In particular, STM has been employed under these conditions to investigate small conjugated oligomers with a size that allows processing in thin films via UHV sublimation: submolecular resolution imaging of these organic surfaces has been attained [34].

A different approach, which is simpler and more compatible with practical and technologically relevant situations, is the processing from solutions. This approach does not suffer from the biggest constraint of UHV, namely the small size of the molecules which can be sublimed due to their poor thermal stability. Consequently it is applicable also to polymers. Nevertheless, a severe limitation is the poor solubility of large conjugated compounds in organic solvents. In this regard, a big effort has been devoted in the last 20 years to the design of large conjugated molecules which would exhibit a good solubility in organic solvents. A notable discovery was that of the precursor route, that can be also called the 'reaction-at-the-surface' route, introduced by Feast and co-workers, which made it possible to process polyacetylenes in films [35]. Another important contribution was the approach of functionalizing the backbone of rod-like polymers with aliphatic side-chains, leading to the so-called 'hairy rods' [36–38]. This strategy also opened new avenues for the functionalization of conjugated (macro)molecules with side-chains bearing electron-withdrawing or electron-donating groups, which makes it possible to tune the electronic properties of the overall material [39, 40].

Two different routes can be followed in order to prepare ordered nanostructures from solutions of soluble compounds: (1) self-assembly at solid–liquid interfaces; and (2) preparation of dry films from solutions, this latter being more in line with the development of working devices. Using both these two methodologies, monodisperse and polydisperse π-conjugated systems have been processed into ordered microstructures and nanostructures on different electrically conducting and insulating flat solid supports.

For all the different approaches discussed so far the choice of the substrate is of pivotal importance. In order to control the growth of highly ordered (macro)molecular structures it is essential to employ substrates with a controlled surface structure, ideally with an atomic flatness extended on the several micrometre scale. In view of this, layered substrates, such as mica or graphite, have been frequently utilized. Alternatively, metallic surfaces have also been used although they possess the disadvantages of requiring to be produced by vacuum processing and needing to be prepared freshly before the adsorbate deposition, since it is not easy to store them for a long time. A new approach was introduced by Hegner and co-workers [41, 42] which was termed 'template stripped gold surfaces' (TSG). These substrates were prepared by:

(i) vacuum sublimation of a 100 nm thick layer of Au on a freshly cleaved mica surface;
(ii) gluing a Si wafer on top of the Au surface; and
(iii) stripping off the Au film that was adjacent to the mica.

This procedure allowed not only improvement of the flatness of the Au surface, but also storage of the mica/Au/Si multilayer for years—performing the stripping just before the deposition of the organic material. Further improvements of these procedures were introduced by growing the Au film on a Si wafer instead of mica [43] and supporting the Au film on an electroplated Ni surface. This latter approach made it possible to increase the stability of the multilayer against different solvents [44]. Recently an Au film, using the TSG approach, was sublimed also on amorphous polymeric masters, allowing tuning of the crystallinity of the interface obtained, keeping the surface roughness very small [45]. This TSG approach can also be extended for the preparation of other metal films such as silver and platinum. In the framework of the improvement of the flatness of the substrate, it is also important to highlight the effort devoted to indium tin oxide, which represents by far the most relevant surface for the fabrication of optoelectronic devices [46]. Among the different treatments that have been tested, oxygen–plasma etching leads to films with higher flatness, higher work-function, and lower sheet resistance.

5.1. Chemisorbed hybrid systems

Making use of chemisorption, it has been possible to self-assemble crystalline monolayers of properly functionalized rod-like conjugated oligomers on metallic surfaces either (i) as a single component or (ii) embedded in a monolayer of saturated alkanethiols.

Trimers of phenylene-ethynylenes were chemisorbed on a Au(111) surface following procedures (i) [47, 48] and (ii) [49]. This latter approach has also been recently employed with oligo-para-phenylene derivatives [50]. Some preliminary results were obtained on short oligomeric derivatives of thiol-end-functionalized polyacetylene chemisorbed on a Au(111) surface, and their electrical characteristics have been compared to those of their saturated derivatives [51, 52]. This revealed a higher resistance of the adlayer composed of saturated derivatives. Although investigations on molecules in films of type (ii) are not easy, the averaged electrical conductivities of these architectures between the two electrodes (STM tip and conductive substrate) have been determined [49].

5.2. Physisorbed hybrid systems

Vacuum-grown π-architectures. Sublimation in a vacuum environment has been used to produce highly ordered films by varying different experimental conditions. The temperature of the substrate during the process of sublimation [53–57] and post-treatments such as thermal annealing [58] turned out to be crucial steps for the improvement of the degree of molecular order on the micrometre scale for oligo-thiophene films grown by sublimation in high vacuum and studied by AFM. Differently from these latter studies on the micrometer scale, STM has been exploited on the molecular scale to provide information on the structure and the dynamics of conjugated materials grown on conductive substrates [34, 59–68]. Making use of this vacuum sublimation procedure, and keeping low deposition rates, layers consisting of monocrystalline domains with lateral sizes on the hundreds of nanometres scale were produced.

Interestingly, the adsorption of sexithiophenes on Au(110) [69] and of polycyclic aromatic hydrocarbons on the Cu(110) [70] surfaces revealed that the molecule–surface interactions are strong enough to induce structural rearrangements in the metallic substrates [70]. These results raise important questions regarding the properties of conjugated molecules grown on

conductive substrates: What type of interaction exists between the adsorbate and the substrate? How strong is it? Can one define it as chemisorption or physisorption? The force between adsorbate and substrate arises predominantly from the gain in enthalpy upon adsorption. This can be pretty high and it increases with the size of the admolecule. As evidence, Umbach and co-workers have been able to show by x-ray photoelectron spectroscopies and programmed thermal desorption measurements that while thienyl [71] and bis-thienyl [72] weakly adsorb on a Ag(111) surface, quarter-thienyl strongly binds to the Ag(111) surface [73, 74]. It is crucial to determine whether the binding is strong enough to induce intramolecular conformational transitions or structural rearrangements of the substrate. In such a case it is most likely that it is higher than the 2 kJ mol $^{-1}$ which is usually assigned to a physisorption process [75].

Submonolayer quantities of conjugated species have been deposited in UHV on metallic surfaces and the tip of a STM has been employed to manipulate single molecules *in situ*, inducing conformational molecular switches [2, 3, 76, 77] (figure 1). This represents a step forward towards the fabrication of molecular tunnel-wired nanorobots [78]. Moreover the manipulation of individual molecules on a conductive substrate allows one to place them in desired positions on the surface. This method was applied to move polycyclic aromatic hydrocarbons (PAHs) to a double atomic step of the Cu(100) surface that could then act as a well-defined electrode. The tip of the STM behaved as a counter-electrode, and in this way the conductivity of the single molecules along the 'conjugated diving board' was probed. The study revealed an exponential decay of the conductivity with the distance from the contact end [79].

Another important advantage of operating in such a controlled UHV atmosphere is the possibility of complementing these types of study with other explorations accomplished with conventional surface science methodologies. In particular, insight into the stoichiometry and the distribution of the electronic levels of conjugated thin films can be obtained by means of photoelectron spectroscopies using x-rays or UV light, respectively [80–84].

UHV sublimation of submonolayer quantities of porphyrin derivatives bearing cyano substituents in different peripheral positions allowed to direct the formation of highly ordered supramolecular nanostructures with targeted shapes and sizes [85].

Following the strategy of the precursor route and making use of high temperatures (about 700 °C), Wöll and Müllen have been able to synthesize on a flat surface a hexa-*peri*-hexabenzocoronene derivative from its physisorbed precursor, namely a substituted hexaphenyl-benzene [86, 87].

The STM tip could be also applied to inject electrons generating electroluminescence. This experiment performed in UHV revealed that a 3 nm thick layer of a poly-para-phenylene-vinylene (PPV) derivative deposited on an Au surface can electroluminesce upon recombination of holes injected by the substrate and electrons injected by the tip, setting a tunnelling current at 100 pA and a STM tip bias of -2.5 V relative to the gold anode (figure 2) [9].

Beyond imaging, a new application of AFM is the conducting probe atomic force microscopy (CPAFM) [88, 89]. It couples nanoscale electrical characterization and topographic imaging using an Au-coated tip to probe the electrical properties and the force interaction with the surface. This methodology has been employed by Frisbie *et al* to explore the electrical properties of micrometre-size doped crystals of sexithiophenes grown by vacuum sublimation on Au and SiO_2 substrates. The vertical and horizontal conductance revealed a non-ohmic behaviour which might arise from an energy barrier to charge injection at the metal–organic interface [89, 90]. In this way the critical role played by the resistance of a grain boundary in the electrical properties of a crystallite was evidenced [90]. Following the same method, more recently a study on the contact properties of a field effect transistor based on single sexithiophene grains was executed. It confirmed that the gain boundaries can be the

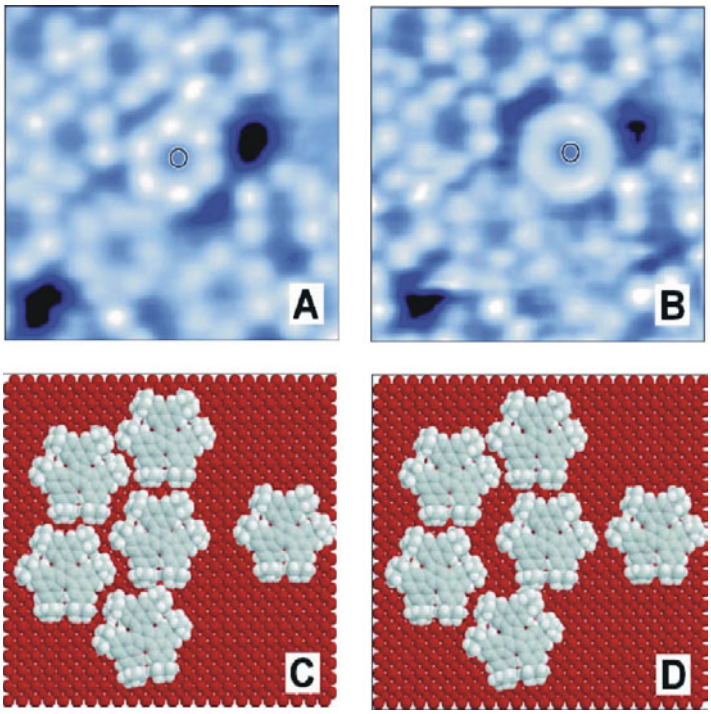

Figure 1. A single-molecule rotor operating within a supramolecular bearing at room temperature. (A), (B) STM images of hexa-*tert*-butyl decacyclene molecules at just below monolayer coverage on Cu(100). (A) In a nanoscopic void, the central molecule is imaged as a six-lobed structure (see the circle) and is immobilized at a high-symmetry site defined by the surrounding molecules. In (B), a lateral translation by one Cu lattice spacing (0.26 nm) shifts the molecule to a lower-symmetry site where it is imaged as a torus, indicating rotation (image area: 5.75 nm by 5.75 nm). (C), (D) Snapshots of the molecular mechanical simulations based on the molecular coordinates taken from the STM data. The central rotor was rotated to compute the rotational barriers in the fixed and rotating states, which were found to be above and below room temperature, respectively [2].

principal bottleneck in charge transport in polycrystalline organic semiconductor films. The energy barrier at the gain boundary has been estimated as 100 meV [91].

5.2.1. Solid–liquid interface. STM investigation at the solid–liquid interfaces is a very practical approach to study at the molecular level ordered adlayers of monodisperse and polydisperse conjugated molecular systems on solid substrates [92–95]. This methodology takes advantage of the tendency of different molecular systems to spontaneously physisorb from solutions on the basal plane of flat solid surfaces. During the STM measurements, which are commonly accomplished employing highly oriented pyrolytic graphite (HOPG) or MoS_2 substrates, the STM tip is immersed in an almost saturated solution in an organic solvent of low polarity. Upon increasing the tunnelling junction impedance, i.e. by changing the tunnelling conditions in STM imaging, it is possible to lift the tip from the substrate. This permits one to switch from the visualization of the substrate lattice to the self-assembled structures of the adlayer, making it possible to calibrate the system with respect to the lattice of the substrate underneath. In this way, by observing the so-called 'Moiré pattern', namely the contrast in the STM image due to the mismatch between the lattices of the admolecule and the one of substrate, a lateral resolution of tenths of ångström can be achieved [93]. It is most important to

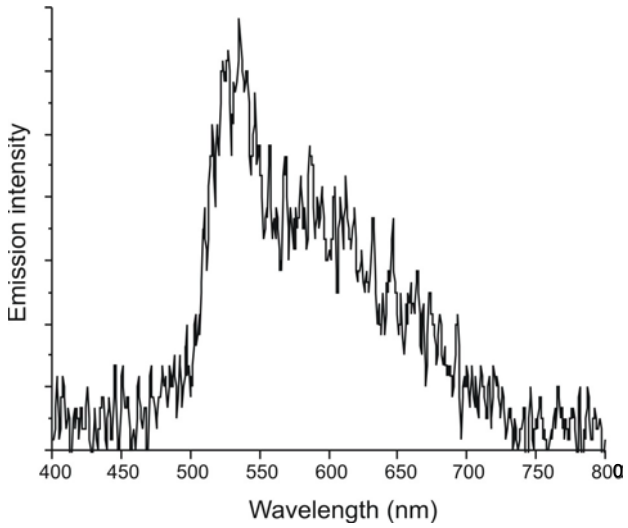

Figure 2. An STM-induced electroluminescence emission spectrum of a PPV film deposited on Au (courtesy of Dr D G Lidzey and Dr S F Alvarado) [9].

point out that the visualized monolayer at this interface is at thermodynamic equilibrium with the 3D supernatant solution. Upon adsorption on the surface the system gains an amount of enthalpy which is proportional to the number of repeat units which are packed on the surface. Consequently it is proportional to the packing density. At the same time the system loses entropy (i) upon reduction of the dimensionality from a 3D to a 2D scenario and (ii) due to the formation of a densely packed monolayer on the surface. This entropy–enthalpy interplay was highlighted by the visualization of a macromolecular fractionation phenomenon of poly-para-phenylene-ethynylene rods at this interface [96]. The study revealed the tendency of both the shorter and the longer chains not to adsorb on the interface. Whilst for the shorter chains the loss in translational entropy is too large, for longer ones the loss in conformational entropy in a densely packed 2D structure is too high, due to their finite persistence length. Following this first visualization of a polydisperse system at the solid–liquid interface [97], the single strands of an alkylated polythiophene derivative were also resolved with STM. This provided evidence of the folding of the single-polymer chains directed by the threefold symmetry of the graphite substrate [98].

It is intriguing to compare the self-assembly behaviour of oligo-thiophenes bearing different side substituents. While the alkyl side-groups induce the formation of lamellae characterized by a staggered arrangement of the single molecules [99–105] (figure 3(a)), the addition of hydrogen-bond-forming groups in the α- and ω-positions of the main chains can be used to design a precise stacking of the functionalized oligo-thiophenes enabling a notable increase of the intermolecular overlap of the π-orbitals [106, 107] (figures 3(b), (c)).

A great deal of activity has also been directed towards molecular systems with a disc-like shape. One class of compounds which has been thoroughly investigated is polycyclic aromatic hydrocarbons (PAHs), which can be regarded as two-dimensional segments of graphite. They are well-defined nano-objects [8, 108–129] with interesting electronic properties [8, 116–121, 125, 127]. During the last few years, soluble derivatives such as alkylated hexa-*peri*-hexabenzocoronenes (HBCs), and larger analogues have been synthesized. From a synthesis point of view, they are extremely versatile compounds that are able to

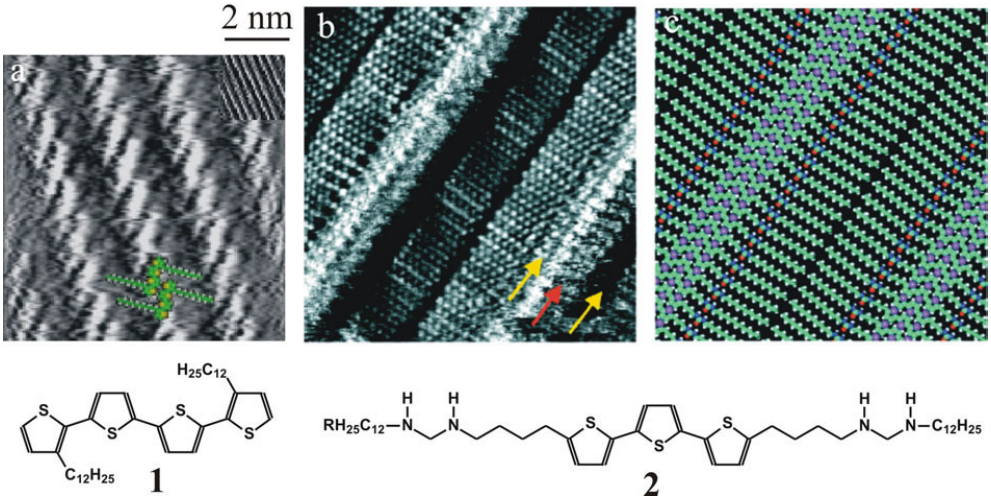

Figure 3. STM images at the graphite–solution interface of (a) **1** in trichlorobenzene (the inset shows an enlargement) [100] and (b) **2** in 1-octanol. The red arrow in (b) indicates the location of the thiophene rings within a lamella [106]. The yellow arrows indicate the location of the urea groups. (c) shows the packing model for (b) [106].

bear different chemical functionalities in their periphery [8, 122–129]. From an electronic viewpoint they are very important, since they exhibit the highest charge-carrier mobility among discotic liquid-crystal-forming molecules [130]. Molecularly resolved STM studies on physisorbed layers of PAHs were carried out both at the graphite–solution interface for alkylated derivatives [8, 119–121, 125, 128] and in dry thin films on conductive substrates for the unsubstituted molecules [129] (see below). The first PAHs which were explored were those of the triphenylene derivative type [119–121, 131], which possess 18 carbon atoms in the aromatic core. Following the recent achievements in the synthesis of larger and larger PAHs, the packing at surfaces of compounds with 42 [8, 128, 129] and 60 carbons [125] in the conjugated core has also been studied. These systems have been found to form two-dimensional crystals where the disc-like molecules lie flat on the basal plane of the conductive substrate. The non-covalent intermolecular interactions among properly substituted HBCs can induce the formation of different patterns on the molecular scale, including dimers and triplets [128]. Very recently, by tuning the side-groups attached symmetrically in the six peripheral positions of the HBC, it has also been possible to extend the crystalline order to the third dimension in the region near to the surface, forming a staircase architecture. This new nanostructure can be of extreme interest for STS (see below), which should allow study of the different physicochemical properties of identical molecules differently coupled with the substrate [27]. In order to solve the dilemma of the low solubility of conjugated molecules in organic solvent, HBCs have been processed in thin films from solution using different procedures. One method which was employed successfully is the reaction-at-the-surface approach, starting from the precursor, namely the hexa-phenyl-benzene. One method used was the one exploited by Wöll et al, based on thermal treatment, which was introduced above [86, 87]. An alternative process started from the visualization of several tens of nanometre-sized 2D crystals of the soluble alkylated precursor at the solid–liquid interface. On this nanostructure the oxidative cyclodehydrogenation reaction was accomplished in the region near to the surface by addition of $FeCl_3$ in CH_3NO_2. Subsequent to carefully rinsing the surface with the pure solvent in order

to wash away all the leftover ions from the reactant, the HBCs monolayers were monitored, proving that the reaction occurred [132].

The reaction-at-the-surface approach has been used also to control the occurrence of the polymerization of the precursor to form polydiacetylene chains on surfaces; as stimuli, light [133] and a voltage applied by the STM [134] have been employed. In both cases the STM imaging has been used to visualize the product of the reaction.

Electron acceptor PAHs such as perylene-3, 4, 9, 10-tetracarboxylic acid dianhydride (PTCDA) and perylene-3, 4, 9, 10-tetracarboxylic acid diimides (PTCDI) were physisorbed at the substrate–solution interface in 1-phenyloctane onto the basal plane of HOPG and MoS_2 into crystalline domains [135]. Identical results were obtained for dry films of the same solutions on the same substrates, just taking the precaution of keeping the substrate at 50 °C for several hours during the adsorption [135].

The formation of stable crystalline monolayers of polycyclic aromatics based on heteroatomic molecular systems including porphyrin and phthalocyanine derivatives has been investigated by Bai and co-workers [136–140]. Upon functionalization of the porphyrins and phthalocyanines with carboxyl groups it was possible to create an extended 2D network on the surface with packing motifs which were driven by the formation of H-bonded networks [140].

Molecular systems with increased complexity, which are more and more synthetically affordable, have also been physisorbed at the solid–liquid interface and visualized with a submolecular resolution. Results include STM explorations on ordered nanostructures of another class of disc-like systems, i.e. macrocycles. Such investigated compounds were based on phenylene-ethynylene [141] segments or thiophene [142, 143] moieties. In the framework of the development of molecular nanowires, these latter are particularly interesting in view of the formation of columnar stacks of macrocycles which coordinate metallic atoms or small molecules in the hollow centre. Also, three-dimensional systems such as [2] catenanes consisting of alternated flexible (saturated) and rigid (unsaturated) moieties were physisorbed into crystalline architectures, which allowed the shedding of further light on the thermodynamics of the physisorption at the solid–liquid interface [144].

5.2.2. Gel–solid interface. Starting from the STM investigation at the solid–liquid interface, very recently a new methodology for the investigation of organic adsorbates was introduced by Samorí *et al* [145]. In this case, upon solvent evaporation a gel was formed which was stable on the substrate surface for several days. As an example, crown ether-functionalized phthalocyanines were investigated under these conditions (figure 4(d)). Submolecular-resolution STM imaging revealed the coexistence of three different nanostructures on an area of some hundreds of square nanometres. A first one (1) arranged 'edge-on', forming lamellae consisting of π–π stacked phthalocyanines, and two (2 and 3) highly ordered 'face-on' hexagonal phases. Since this gel–graphite interface is very durable, it becomes possible to perform STM measurements continuously for several days with the tip immersed in the gel. Moreover, the slow dynamics of the single molecules at this interface allowed one not only to follow the path of a single molecule on a timescale of several hours, but also to readily manipulate the molecular adsorbate with a precision on the molecular scale. In this set of experiments, after having 'read' the surface (figures 4(a), (d)), the tip of the STM was used in a invasive mode to 'write' information on the molecular scale (figure 4(b)). This has been done by reducing the tunnelling gap impedance, in this way inducing a mechanochemical switch from the 'face-on' to the 'edge-on' packing. Going back to the non-invasive measurement conditions, the surface was 'read' again and the switching which occurred in area 4 was monitored (figures 4(c), (e)).

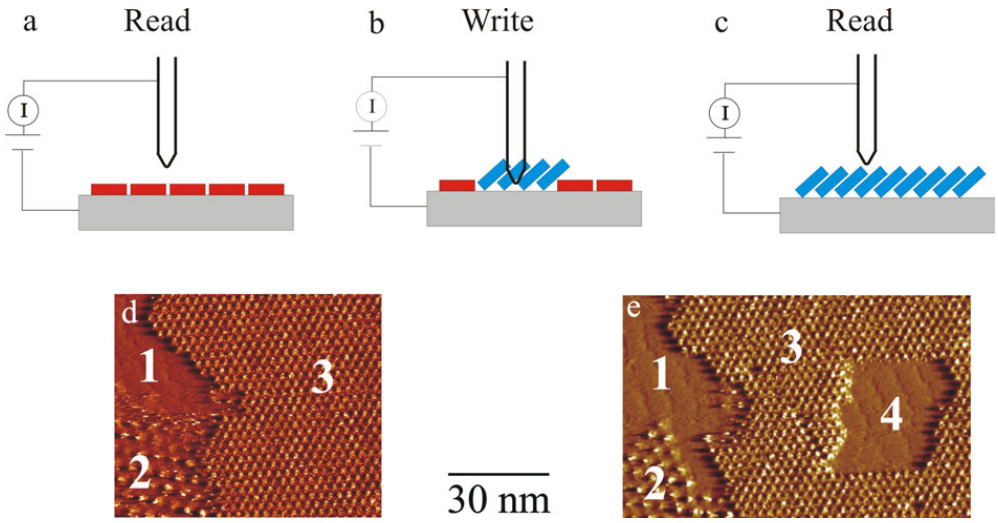

Figure 4. Schematic diagrams showing the STM tip being used to (a) 'read a surface', (b) 'write a surface', and (c) 'read a surface' again. The STM images were recorded at the gel–HOPG interface: (d) reading the surface before the manipulation; (e) reading the surface after the manipulation. The area indicated by 4 in (e) has been manipulated by inducing a mechanochemical switch from the 'face-on' hexagonally packed structure to the 'edge-on' lamella architecture [145].

6. Scanning tunnelling spectroscopy: beyond imaging

Besides imaging, the STM provides a viable pathway to perform spectroscopical investigations on single molecules using the STS mode [7, 8, 12, 146]. For this the tip is 'frozen' at a well-specified distance from the sample surface (position) and $\mathrm{d}I/\mathrm{d}U$ is sampled as a function of voltage (U) (in a selected range, typically within -2 and +2 V). The resulting characteristic $(\mathrm{d}I/\mathrm{d}U) = f(U)$ can usually be interpreted in terms of the electronic density of states [147]. Several studies on organic layers have been accomplished in UHV and at solid–liquid interfaces. The major difficulties in experiments of this type are related to sample instabilities during the measurements.

For the case of UHV, studies on single copper phthalocyanines by Gimzewski *et al* [7] and later by Dekker *et al* [148] revealed asymmetric $I(U)$ traces, namely an enhanced current at negative sample bias, attributed to a resonant tunnelling through the HOMO of the CuPc. The HOMO–LUMO gap of the Pc was not observed, however. Likewise, studies on vanadyl-derivatized Pcs on Au(111) have shown strongly asymmetric $I(U)$ curves because of an enhanced tunnelling current at positive sample bias [149, 150]. In this case the tunnelling occurred through the LUMO. STS explorations have also been carried out as a function of the distance between tip and surface on chemisorbed monolayers of α, α'-xylyl dithiol on gold [151]. On increasing the tip–surface distance, the $I(U)$ curves become asymmetric. Similar results have been obtained on crystalline monolayers of coronene grown by sublimation on HOPG in UHV [152]. The HOMO–LUMO gap, although smaller than the calculated value for an isolated molecule, increases with the size of the tip–sample gap.

The combination of STS and optical absorption measurements was used to determine the exciton binding of PPV and polyfluorene derivatives [153]. The STS can be used also to determine the band gap for a conjugated polymer film of PPV. The data obtained are in good agreement with optical spectroscopy measurements [154]. Exploiting STS and UPS

on unsubstituted HBCs sublimed in UHV on Au(111), comparable results for the electronic structure of the occupied states have been sampled. Also in this case, the measured band gap is in accordance with the one determined from optical absorption [83].

Only a few STS studies have been reported on organic molecules at the liquid/solid interface. The use of STS under these conditions was employed first by Rabe and co-workers in order to compare the STS plots of the saturated and unsaturated moieties in a single-alkylated hexa-*peri*-hexabenzocoronene physisorbed at the graphite–solution interface. While the $I(U)$ characteristics of the aliphatic side-chains are symmetric, those of the conjugated core moieties are asymmetric [8]. Under the same solid–liquid interface conditions, metalloporphyrin derivatives assembled on gold surfaces have been investigated with STS. Asymmetric $I(U)$ spectra have also been found due to an increase in tunnelling current at high negative sample bias. This increase is explained by tunnelling via oxidized states on the molecule [155]. Again, asymmetric traces have been recorded on self-assembled monolayers of thiol-functionalized aromatic moieties in air [156]. The molecules have been found to act as potential barriers to electron transmission. The barrier is trapezoidal when the molecule has a permanent dipole moment (normal to the basal plane of the Au surface), in accordance with the asymmetric $I(U)$ traces [157].

7. Solution-grown dry films

SFM has been used primarily for characterizing the structures of organic micro- and nano-architectures under various boundary conditions on electrically conductive or insulating substrates. The dominant type of intermolecular interaction that is observed between conjugated (macro)molecules is π–π stacking. This type of force has been utilized for the generation of micrometre long nanoribbon architectures with a molecular cross-section via the self-assembly of functionalized homopolymeric derivatives of para-phenylene-ethynylene (PPE) [97]. The growth into nanoribbons can be explained with the maximization of the intermolecular π–π stacking. These highly ordered molecular nanostructures, after being doped, are promising candidates for the development of molecular nanowires to be interfaced to gold nanoelectrodes prepared by lithographic routes. Similar nanoribbons based on PPE derivatives have also been produced by Bunz and co-workers [158].

Related to these findings, very fine data have been obtained on the self-assembly of block-copolymers which are based on a rod-like conjugated segment covalently linked to a coiled strand. SFM investigations addressed to polymeric PPEs [159] or para-phenylenes [160] as conjugated segments covalently linked to flexible polydimethylsiloxane or polyethylene oxide chains were carried out by Lazzaroni and co-workers. These studies revealed that, similarly to the case for the aforementioned homopolymers, the molecules self-assemble into nanoribbons on insulating surfaces. This type of order has been found on copolymers made with a saturated and an unsaturated block, where the conjugated blocks are at least as long as the saturated ones. Simply by increasing the length of the coiled chain by one order of magnitude, it was possible to obtain a different molecular arrangement governed by the interactions between the flexible strands. Particularly on this type of composite film, the phase imaging in the Tapping Mode is of extreme importance. This procedure, which allowed probing of the different mechanical properties of an adsorbate in different locations, is ideal for visualizing different phases on the sample surface.

Larger anisotropic arrangements of amphiphilic polythiophenes have been transferred to the surface with a Langmuir trough and visualized with AFM. One obtains wires with lengths on the micrometre scale, widths of 60 nm, and heights of 10–15 nm [161]. A room temperature conductivity of these architectures of 40 S cm^{-1} was quantified by four-point

probe measurements [161]. Similar approaches have been employed to grow π–π stacked micrometre long rod-like structures of amphiphilic phthalocyanine derivatives with a molecular cross-section which was visualized both with AFM and STM [162–164].

SFM in dynamic modes (including Tapping Mode and non-contact mode) has been an important tool in investigating nanostructures based on conjugated dendrimers. Müllen's phenylene-based dendrimers [165] have been studied both by arranging them in thin continuous films physisorbed on graphite and also as isolated molecules adsorbed on flat surfaces such as mica. In the first case nanorods have been visualized with a resolution which allowed to resolve the structure on the few-nanometres scale [166, 167]. In the latter case, by using the pulsed force mode atomic microscope [168] it recently became possible to gain insight into the adhesion on mica of different phenylene-based dendrimers with increasing generation either with [169] or without [170] carboxyl groups in the outer rim.

8. Discussion and open issues

Scanning probe microscopy techniques have certainly broadened the scope for approaching and controlling the properties of single molecules. The first person who dared to think so small was Richard Feynman in 1959, who, in his famous talk entitled 'There's Plenty of Room at the Bottom [171], said: 'I can hardly doubt that when we have some control of the arrangement of things on a small scale we will get an enormously greater range of possible properties that substances can have, and of different things that we can do'. Different important topics still need to be tackled to improve the capability of controlling the physicochemical properties of single molecules as well as of supramolecular architectures. Just combining the *bottom-up* approach with the *top-down* one can improve the properties and the accessibility of nanometre-sized structures, opening perspectives for the development of nanometre-scale devices.

A key goal is to enhance the *processability* of conjugated molecules from solutions, since it is clear that the limitation of UHV sublimation in the size of the molecules which can be deposited is difficult to overcome. Emphasis should be given to casting more light on the process of the adsorption on a surface and its effect on the properties of the adsorbing molecule and of the substrate. For example, a key issue is the perturbation of the electronic states of the adsorbing molecules due to the interaction with the electronic states of the substrate. In the framework of the development of prototypes of molecular wires, an important problem that needs to be solved is that of the reproducibility of the contact between the electrodes and the molecular arrangements with a precision on the atomic scale. Moreover, with the increasing degree of complexity of molecular and supramolecular species that are nowadays available, new avenues of exploration need to followed. Under these conditions the development of devices with tuned performances can be foreseen.

In view of the development of *photovoltaic devices*, it is extremely interesting to prepare thin films consisting of different components of electron-rich and electron-poor conjugated compounds [172–175]. Very recently, the groups of Friend and Müllen revealed that films which convey vertically segregated hexa-*peri*-hexabenzocoronene (HBC) and perylene derivatives can exhibit high photovoltaic response with high external quantum efficiencies of more than 34% near $\lambda = 490$ nm. These efficiencies result from efficient photoinduced charge transfer between the HBC and the perylene, as well as from effective transport of charges through vertically segregated perylene and HBC π-systems [176]. Following this seminal work, efforts might be devoted towards the control of the self-assembly of multicomponent architectures into highly ordered arrangements.

The path towards the development of working *molecular nanowire* devices appears still quite long and requires solutions to some basic problems such as the improvement of the

stiffness of the molecules composing the wire, and the possibility of processing a structurally stable *doped* conjugated wire. Consequently, it will be very important to focus attention towards the synthesis of shape-persistent structurally defined self-doped polymers. In addition, it will be of fundamental importance to compare the electrical properties of doped single molecules and their supramolecular architectures in order to cast light on the role played by interchain hopping in the conductivity of organic nanostructures.

9. Conclusions

STM and SFM techniques are undoubtedly established stars in the firmament of surface science. Given their capability to probe physicochemical properties on a wide range of scan lengths—including the structural and electronic characterization of organic thin films—they represent invaluable tools for present and future research in the fertile field of molecular electronics.

Acknowledgments

It is a great pleasure to acknowledge the very fruitful long term collaborations with the groups of Professor Dr K Müllen (MPI-Mainz) and Professor Dr R J M Nolte (University of Nijmegen). We are also indebted to Professor Dr J-M Lehn and Dr A Wei (University Louis Pasteur—Strasbourg) for their support in the thiol-functionalized oligo-acetylene project. Financial support from the EU through the TMR network SISITOMAS is acknowledged. PS thanks the EU for a Marie Curie fellowship. We would also like to thank a referee for helpful comments.

References

[1] Yazdani A and Lieber C M 1999 *Nature* **401** 227–30
[2] Gimzewski J K and Joachim C 1999 *Science* **283** 1683–8
[3] Jung T A, Schlittler R R, Gimzewski J K, Tang H and Joachim C 1996 *Science* **271** 181–4
[4] Stabel A, Heinz R, De Schryver F C and Rabe J P 1995 *J. Phys. Chem.* **99** 505
[5] Heinz R, Stabel A, Rabe J P, Wegner G, De Schryver F C, Corens D, Dehaen W and Süling C 1994 *Angew. Chem., Int. Edn Engl.* **33** 2080
[6] Abdel-Mottaleb M M S, De Feyter S, Gesquière A, Sieffert M, Klapper M, Müllen K and De Schryver F C 2001 *Nano Lett.* **1** 353–9
[7] Gimzewski J K, Stoll E and Schlittler R R 1987 *Surf. Sci.* **181** 267–77
[8] Stabel A, Herwig P, Müllen K and Rabe J P 1995 *Angew. Chem., Int. Edn Engl.* **34** 1609–11
[9] Lidzey D, Bradley D D C, Alvarado S F and Seidler P F 1997 *Nature* **386** 135
[10] Binnig G, Rohrer H, Gerber C and Weibel E 1982 *Helv. Phys. Acta* **55** 726
[11] Binnig G, Rohrer H, Gerber C and Weibel E 1982 *Appl. Phys. Lett.* **40** 178
[12] Wiesendanger R 1998 *Scanning Probe Microscopy and Spectroscopy, Methods and Applications* (Cambridge: Cambridge University Press)
[13] Binnig G, Quate C F and Gerber C 1986 *Phys. Rev. Lett.* **56** 930
[14] Rugar D and Hansma P K 1990 *Phys. Today* 23–30
[15] Bustamante C and Keller D 1995 *Phys. Today* 32–8
[16] Takano H, Kenseth J R, Wong S S, O'Brien J C and Porter M D 1999 *Chem. Rev.* **99** 2845
[17] Bucher J P, Santesson L and Kern K 1994 *Langmuir* **10** 979
[18] Vekilov P G and Alexander J I D 2000 *Chem. Rev.* **100** 2061–89
[19] Gimzewski J K and Möller R 1987 *Phys. Rev.* B **36** 1284
[20] Hansma P K and Tersoff J 1987 *J. Appl. Phys.* **61** R1
[21] Sautet P 1997 *Chem. Rev.* **97** 1097–116
[22] Biscarini F, Bustamante C and Kenkre V M 1995 *Phys. Rev.* B **51** 11 089–102
[23] Lazzaroni R, Calderone A, Brédas J L and Rabe J P 1997 *J. Chem. Phys.* **107** 99
[24] Orlandi G, Troisi A and Zerbetto F 1999 *J. Am. Chem. Soc.* **121** 5392
[25] Yajima A and Tsukada M 1996 *Surf. Sci.* **366** L715

[26] Lang N D 1985 *Phys. Rev. Lett.* **55** 230
[27] Samorí P, Fechtenkötter A, Jäckel F, Böhme T, Müllen K and Rabe J P 2001 *J. Am. Chem. Soc.* **123** 11 462–7
[28] Delamarche E, Michel B, Biebuyck H A and Gerber C 1996 *Adv. Mater.* **8** 719
[29] Zhong Q, Inniss D and Elings V 1993 *Surf. Sci.* **290** L688
[30] Tamayo J and Garcia R 1996 *Langmuir* **12** 4430
[31] Leclere P, Lazzaroni R, Brédas J L, Yu J M, Dubois P and Jerome R 1996 *Langmuir* **12** 4317
[32] Finot M O and McDermot M T 1997 *J. Am. Chem. Soc.* **119** 8564
[33] Stocker W, Karakaya B, Schürmann B L, Rabe J P and Schlüter A D 1998 *J. Am. Chem. Soc.* **120** 7691
[34] Forrest S R 1997 *Chem. Rev.* **97** 1793–896
[35] Feast W J, Parker D, Winter J N, Bott D C and Walker S N 1985 *Electronic Properties of Polymers and Related Compounds (Springer Series in Solid-State Science vol 63)* ed H Kuzmany, M Mehring and S Roth (Heidelberg: Springer) p 45
[36] Orthmann E and Wegner G 1986 *Angew. Chem., Int. Edn* **25** 1105–7
[37] Ballauff M 1989 *Angew. Chem., Int. Edn* **28** 253
[38] Rehahn M, Schlüter A D, Wegner G and Feast J 1989 *Polymer* **30** 1054–60
[39] Braun D and Heeger A J 1991 *Appl. Phys. Lett.* **58** 1982–4
[40] Greenham N C, Moratti S C, Bradley D D C, Friend R H and Holmes A B 1993 *Nature* **365** 628–30
[41] Hegner M, Wagner P and Semenza G 1993 *Surf. Sci.* **291** 39
[42] Wagner P, Hegner M, Güntherodt H J and Semenza G 1995 *Langmuir* **10** 3867
[43] Stamou D, Gourdon D, Liley M, Burnham N A, Kulik A, Vogel H and Duschl C 1997 *Langmuir* **13** 2425
[44] Samorí P, Diebel J, Löwe H and Rabe J P 1999 *Langmuir* **15** 2592
[45] Diebel J, Löwe H, Samorí P and Rabe J P 2001 *Appl. Phys.* A **73** 273–9
[46] Kim J S, Granström M, Friend R H, Johansson N, Salaneck W R, Daik R, Feast W J and Cacialli F 1998 *J. Appl. Phys.* **84** 6859–70
[47] Dhirani A A, Zehner R W, Hsung R P, Guyot-Sionnest P and Sita L R 1996 *J. Am. Chem. Soc.* **118** 3319–20
[48] Dhirani A, Lin P H, GuyotSionnest P, Zehner R W and Sita L R 1997 *J. Chem. Phys.* **106** 5249–53
[49] Bumm L A, Arnold J J, Cygan M T, Dunbar T D, Burgin T P, Jones L II, Allara D L, Tour J M and Weiss P S 1996 *Science* **271** 1705–7
[50] Ishida T, Mizutani W, Choi N, Akiba U, Fujihira M and Tokumoto H 2000 *J. Phys. Chem.* B **104** 11 680–8
[51] Samorí P 2000 *PhD Thesis* Humboldt University Berlin (available at http://dochost.rz.hu-berlin.de/dissertationen/samori-paolo-2000-10-24 /PDF/Samori.pdf)
[52] Wei A, Samorí P, Rabe J P and Lehn J M, unpublished
[53] Biscarini F, Zamboni R, Samorí P, Ostoja P and Taliani C 1995 *Phys. Rev.* B **52** 14 868–77
[54] Biscarini F, Samorí P, Greco O and Zamboni R 1997 *Phys. Rev. Lett.* **78** 2389–92
[55] Müller E and Ziegler C 2000 *J. Mater. Chem.* **10** 47–53
[56] Marks R N, Biscarini F, Zamboni R and Taliani C 1995 *Europhys. Lett.* **32** 523–8
[57] Muccini M, Murgia M, Biscarini F and Taliani C 2001 *Adv. Mater.* **13** 355–8
[58] Viville P, Lazzaroni R, Brédas J L, Moretti P, Samorí P and Biscarini F 1998 *Adv. Mater.* **10** 57–60
[59] Ludwig C, Gompf B, Glatz W, Petersen J, Eisenmenger W, Möbus M, Zimmermann U and Karl N 1992 *J. Phys.: Condens. Matter* **86** 397–404
[60] Schmitz-Hübsch T, Fritz T, Staub R, Back A, Armstrong N R and Leo K 1999 *Surf. Sci.* **437** 163–72
[61] Fritz T, Hoffmann M, Schmitz-Hübsch T and Leo K 1998 *Mol. Cryst. Liq. Cryst.* **314** 279–84
[62] Glöckler K, Seidel C, Soukopp A, Sokolowski M, Umbach E, Bohringer M, Berndt R and Schneider W D 1998 *Surf. Sci.* **405** 1–20
[63] Schmitz-Hübsch T, Fritz T, Sellam F, Staub R and Leo K 1997 *Phys. Rev.* B **55** 7972–6
[64] Seidel C, Awater C, Liu X D, Ellerbrake R and Fuchs H 1997 *Surf. Sci.* **371** 123–30
[65] Kendrick C and Kahn A 1998 *Appl. Surf. Sci.* **123** 405–11
[66] Seidel C, Schafer A H and Fuchs H 2000 *Surf. Sci.* **459** 310–22
[67] Umbach E, Glöckler K and Sokolowski M 1998 *Surf. Sci.* **404** 20–31
[68] Böhringer M, Schneider W D, Berndt R, Glöckler K, Sokolowski M and Umbach E 1998 *Phys. Rev.* B **57** 4081–7
[69] Prato S, Floreano L, Cvetko D, De Renzi V, Morgante A, Modesti S, Biscarini F, Zamboni R and Taliani C 1999 *J. Phys. Chem.* B **103** 7788–95
[70] Schunack M, Petersen L, Kühnle A, Lægsgaard E, Stensgaard I, Johannsen I and Besenbacher D 2001 *Phys. Rev. Lett.* **86** 456–9
[71] Baumgärtner K M, Volmer-Übing M, Taborski J, Bäuerle P and Umbach E 1991 *Ber. Bunsenges. Phys. Chem.* **95** 1488

[72] Vaterlein P, Schmelzer M, Taborski J, Krause T, Viczian F, Bassler M, Fink R, Umbach E and Wurth W 2000 *Surf. Sci.* **452** 20–32
[73] Li R, Bäuerle P and Umbach E 1995 *Surf. Sci.* **333** 100–4
[74] Soukopp A, Seidel C, Li R, Bassler M, Sokolowski M and Umbach E 1996 *Thin Solid Films* **285** 343–6
[75] Atkins P W 1994 *Physical Chemistry* (Oxford: Oxford University Press)
[76] Gimzewski J K, Joachim C, Schlittler R R, Langlais V, Tang H and Johannsen I 1998 *Science* **281** 531–3
[77] Moresco F, Meyer G, Rieder K H, Tang H, Gourdon A and Joachim C 2001 *Phys. Rev. Lett.* **86** 672–5
[78] Moresco F, Meyer G, Rieder K H, Tang H, Gourdon A and Joachim C 2001 *Phys. Rev. Lett.* **87** 8302
[79] Langlais V J, Schlittler R R, Tang H, Gourdon A, Joachim C and Gimzewski J K 1999 *Phys. Rev. Lett.* **83** 2809–12
[80] Keil M, Samorí P, dos Santos D A, Kugler T, Stafström S, Brand J D, Müllen K, Brédas J L, Rabe J P and Salaneck W R 2000 *J. Phys. Chem.* B **104** 3967–75
[81] Samorí P, Keil M, Friedlein R, Birgerson J, Watson M, Müllen K, Salaneck W R and Rabe J P 2001 *J. Phys. Chem.* B **105** 11 114–19
[82] Scudiero L, Barlow D E, Mazur U and Hipps K W 2001 *J. Am. Chem. Soc.* **123** 4073–80
[83] Proehl H, Toerker M, Sellam F, Fritz T, Leo K, Simpson C and Müllen K 2001 *Phys. Rev.* B **63** 205409
[84] Salaneck W R, Stafström S and Brédas J L 1996 *Conjugated Polymer Surfaces and Interfaces* (Cambridge: Cambridge University Press)
[85] Yokoyama T, Yokoyama S, Kamikado T, Okuno Y and Mashiko S 2001 *Nature* **413** 619–21
[86] Weiss K, Beernick G, Dötz F, Birkner A, Müllen K and Wöll C H 1999 *Angew. Chem.* **111** 3974–8
Weiss K, Beernick G, Dötz F, Birkner A, Müllen K and Wöll C H 1999 *Angew. Chem., Int. Edn Engl.* **38** 3748–52
[87] Beerninck G, Gunia M, Dötz F, Öström H, Weiss K, Müllen K and Wöll C 2001 *Chem. Phys. Chem.* **2** 317–20
[88] Dai H, Wong E W and Lieber C M 1996 *Science* **272** 523
[89] Loiacono M J, Granstrom E L and Frisbie C D 1998 *J. Phys. Chem.* B **102** 1679–88
[90] Kelley T W, Granstrom E L and Frisbie C D 1999 *Adv. Mater.* **11** 261–4
[91] Kelley T W and Frisbie C D 2001 *J. Phys. Chem.* B **105** 4538–40
[92] McGonical G C, Bernhardt R H and Thomson D J 1990 *Appl. Phys. Lett.* **57** 28–30
[93] Rabe J P and Buchholz S 1991 *Science* **253** 424–7
[94] Giancarlo L C and Flynn G W 2000 *Acc. Chem. Res.* **33** 492–501
[95] De Feyter S, Hofkens J, Van der Auweraer M, Nolte R J M, Müllen K and De Schryver F C 2001 *Chem. Commun.* 585–92
[96] Samorí P, Severin N, Müllen K and Rabe J P 2000 *Adv. Mater.* **12** 579–82
[97] Samorí P, Francke V, Müllen K and Rabe J P 1999 *Chem. Eur. J.* **5** 2312–17
[98] Mena-Osteritz E, Meyer A, Langeveld-Voss B M W, Janssen R A J, Meijer E W and Bäuerle P 2000 *Angew. Chem., Int. Edn* **39** 2680–4
[99] Stabel A and Rabe J P 1994 *Synth. Met.* **67** 47–53
[100] Bäuerle P, Fischer T, Bidlingmaier B, Stabel A and Rabe J P 1995 *Angew. Chem., Int. Edn Engl.* **34** 303–7
[101] Stecher R, Gompf B, Münter J R S and Effenberger F 1999 *Adv. Mater.* **11** 927–31
[102] Stecher R, Drewnick F and Gompf B 1999 *Langmuir* **15** 6490–4
[103] Azumi R, Götz G and Bäuerle P 1999 *Synth. Met.* **101** 569–72
[104] Vollmer M S, Effenberger F, Stecher R, Gompf B and Eisenmenger W 1999 *Chem. Eur. J.* **5** 96–101
[105] Azumi R, Gotz G, Debaerdemaeker T and Bäuerle P 2000 *Chem. Eur. J.* **6** 735–44
[106] Gesquière A *et al* 2000 *Langmuir* **16** 20 385–91
[107] Gesquière A, De Feyter S, De Schryver F C, Schoonbeek F, van Esch J, Kellogg R M and Feringa B L 2001 *Nano Lett.* **1** 201–6
[108] Clar E 1952 *Aromatische Kohlenwasserstoffe: Polycyclische Systeme* (Berlin: Springer)
[109] Clar E 1972 *The Aromatic Sextet* (London: Wiley)
[110] Diederich F and Rubin Y 1992 *Angew. Chem., Int. Edn Engl.* **31** 1101–23
[111] Faust R 1995 *Angew. Chem., Int. Edn Engl.* **34** 1429–32
[112] Hudgins D M and Allamandola L J 1995 *J. Phys. Chem.* **99** 3033–46
[113] Scott L T, Cheng P C, Hashemi M M, Bratcher M S, Meyer D T and Warren H B 1997 *J. Am. Chem. Soc.* **119** 10 963–8
[114] Tong L, Lau H, Ho D M and Pascal R A Jr 1998 *J. Am. Chem. Soc.* **120** 6000–6
[115] Debad J D and Bard A J 1998 *J. Am. Chem. Soc.* **120** 2476–7
[116] Adam D, Schuhmacher P, Simmerer J, Häussling L, Siemensmeyer K, Etzbach K H, Ringsdorf H and Haarer D 1994 *Nature* **371** 141–3

[117] Simmerer J *et al* 1996 *Adv. Mater.* **8** 815–19
[118] van de Craats A M, Warman J M, de Haas M P, Adam D, Simmerer J, Haarer D and Schuhmacher P 1996 *Adv. Mater* **8** 823–6
[119] Askadskaya L, Boeffel C and Rabe J P 1993 *Ber. Bunsenges. Phys. Chem.* **97** 517–21
[120] Gabriel J C, Larsen N B, Larsen M, Harrit N, Pedersen J S, Schaumburg K and Bechgaard K 1996 *Langmuir* **12** 1690–2
[121] Charra F and Cousty J 1998 *Phys. Rev. Lett.* **80** 1682–5
[122] Goddard R, Haenel M W, Herndon W C, Krüger C and Zander M 1995 *J. Am. Chem. Soc.* **117** 30–41
[123] Herwig P, Kayser C W, Müllen K and Spiess H W 1996 *Adv. Mater.* **8** 510–13
[124] Müller M, Kübel Ch and Müllen K 1998 *Chem. Eur. J.* **4** 2099–109
[125] Iyer V S, Yoshimura K, Enkelmann V, Epsch R, Rabe J P and Müllen K 1998 *Angew. Chem., Int. Edn* **37** 2696–9
[126] Fechtenkötter A, Saalwächter K, Harbison M A, Müllen K and Spiess H W 1999 *Angew. Chem., Int. Edn* **38** 3039–42
[127] van de Craats A M, Warman J M, Fechtenkötter A, Brand J D, Harbison M A and Müllen K 1999 *Adv. Mater.* **11** 1469–72
[128] Ito S, Wehmeier M, Brand J D, Kübel Ch, Epsch R, Rabe J P and Müllen K 2000 *Chem. Eur. J.* **6** 4327–42
[129] Schmitz-Hübsch T, Sellam F, Staub R, Törker M, Fritz T, Kübel Ch, Müllen K and Leo K 2000 *Surf. Sci.* **445** 358–67
[130] van de Craats A M and Warman J M 2001 *Adv. Mater.* **13** 130
[131] Wu P, Zeng Q, Xu S, Wang C, Yin S and Bai C L 2001 *Chem. Phys. Chem.* **2** 750–4
[132] Samorí P, Simpson C, Müllen K and Rabe J P 2002 *Langmuir* **18** 4183
[133] Grim P C M, De Feyter S, Gesquière A, Vanoppen P, Rucker M, Valiyaveettil S, Moessner G, Müllen K and De Schryver F C 1997 *Angew. Chem., Int. Edn* **36** 2601–3
[134] Okawa Y and Aono M 2001 *Nature* **409** 683–4
[135] Kaneda Y, Stawasz M E, Sampson D L and Parkinson B A 2001 *Langmuir* **17** 6185–95
[136] Qiu X H, Wang C, Yin S X, Zeng Q D, Xu B and Bai C L 2000 *J. Phys. Chem.* B **104** 3570–4
[137] Qiu X H, Wang C, Zeng Q D, Xu B, Yin S X, Wang H N, Xu S D and Bai C L 2000 *J. Am. Chem. Soc.* **122** 5550–6
[138] Xu B, Yin S X, Wang C, Qiu X H, Zeng Q D and Bai C L 2000 *J. Phys. Chem.* B **104** 10 502–5
[139] Lei S B, Wang C, Yin S X and Bai C L 2001 *J. Phys. Chem.* B **105** 12 272–7
[140] Lei S B, Wang C, Yin S X, Wang H N, Xi F, Liu H W, Xu B, Wan L J and Bai C L 2001 *J. Phys. Chem.* B **105** 10 838–41
[141] Höger S, Bonrad K, Mourran A, Beginn U and Möller M 2001 *J. Am. Chem. Soc.* **123** 5651–9
[142] Krömer J, Rios-Carreras I, Fuhrmann G, Musch C, Wunderlin M, Debaerdemaeker T, Mena-Osteritz E and Bäuerle P 2000 *Angew. Chem.* **112** 3623–8
[143] Mena-Osteritz E and Bäuerle P 2001 *Adv. Mater.* **13** 243–6
[144] Samorí P, Jäckel F, Godt A and Rabe J P 2001 *Chem. Phys. Chem.* **2** 461–4
[145] Samorí P, Engelkamp H, de Witte P, Rowan A E, Nolte R J M and Rabe J P 2001 *Angew. Chem., Int. Edn* **40** 2348–50
[146] Feenstra R M 1994 *Surf. Sci.* **299–300** 965
[147] Slonczewski J C 1989 *Phys. Rev.* B **39** 6995–7002
[148] Dekker C, Tans S J, Oberndorff B, Meyer R and Venema L C 1997 *Synth. Met.* **84** 853–4
[149] Barlow D E and Hipps K W 2000 *J. Phys. Chem.* B **104** 5993–6000
[150] Hipps K W, Barlow D E and Mazur U 2000 *J. Phys. Chem.* B **104** 2444–7
[151] Datta S, Tian W, Hong S, Reifenberger R, Henderson J I and Kubiak C P 1997 *Phys. Rev. Lett.* **79** 2530–3
[152] Walzer K, Sternberg M and Hietschold M 1998 *Surf. Sci.* **415** 376–84
[153] Alvarado S F, Seidler P F, Lidzey D G and Bradley D D C 1998 *Phys. Rev. Lett.* **81** 1082–5
[154] Rinaldi R, Cingolani R, Jones K M, Baski A A and Morkoc J 2001 *Phys. Rev.* B **63** 075311
[155] Han W, Durantini E N, Moore T A, Moore A L, Gust D, Rez P, Leatherman G, Seely G R, Tao N and Lindsay S M 1997 *J. Phys. Chem.* B **101** 10 719–25
[156] Onipko A I, Berggren K F, Klymenkko Yu O, Malysheva L I, Rosink J J W M, Geerligs L J, van der Drift E and Radelaar S 2000 *Phys. Rev.* B **61** 11 118–24
[157] Rosink J J W M, Blauw M A, Geerligs L J, van der Drift E and Radelaar S 2000 *Phys. Rev.* B **62** 10 459–66
[158] Perahia D, Traiphol R and Bunz U H F 2001 *Macromolecules* **34** 151–5
[159] Leclere P, Calderone A, Marsitzky D, Francke V, Geerts Y, Mullen K, Brédas J L and Lazzaroni R 2000 *Adv. Mater.* **12** 1042–6

[160] Leclere P, Parente V, Brédas J L, Francois B and Lazzaroni R 1998 *Chem. Mater.* **10** 4010–14
[161] Bjørnholm T, Hassenkam T, Greve D R, McCullough R D, Jazaraman M, Savoy S M, Jones C E and McDevitt J T 1999 *Adv. Mater.* **11** 1218–21
[162] Smolenyak P, Peterson R, Nebesny K, Törker M, O'Brien D F and Armstrong N R 1999 *J. Am. Chem. Soc.* **121** 8628–36
[163] Zangmeister A P, Smolenyak P E, Drager A S, O'Brien D F and Armstrong N R 2001 *Langmuir* **17** 7071–8
[164] Drager A S, Zangmeister A P, Armstrong N R and O'Brien D F 2001 *J. Am. Chem. Soc.* **123** 3595–6
[165] Berresheim A J, Müller M and Müllen K 1999 *Chem. Rev.* **99** 1747–86
[166] Loi S, Wiesler U M, Butt H J and Mullen K 2000 *Chem. Commun.* 1169–70
[167] Loi S, Wiesler U M, Butt H J and Mullen K 2001 *Macromolecules* **34** 3661–71
[168] Rosa-Zeiser A, Weilandt E, Weilandt H and Marti O 1997 *Meas. Sci. Technol.* **8** 1333
[169] Zhang H, Grim P C M, Vosch T, Wiesler U M, Berresheim A J, Müllen K and De Schryver F C 2000 *Langmuir* **16** 9294–8
[170] Zhang H, Grim P C M, Foubert P, Vosch T, Vanoppen P, Wiesler U M, Berresheim A J, Müllen K and De Schryver F C 2000 *Langmuir* **16** 9009–14
[171] Feynman R 1959 *Lecture at the Annual Meeting of the American Physical Society (California Institute of Technology, Dec. 1959)*
[172] Halls J J M, Walsh C A, Greenham N C, Marseglia E A, Friend R H, Moratti S C and Holmes A B 1995 *Nature* **376** 498–500
[173] Sariciftci N S 1999 *Curr. Opin. Solid State Mater. Sci.* **4** 373–8
[174] Dittmer J J *et al* 2000 *Sol. Energy Mater. Sol. Cells* **6** 53–61
[175] Eckert J-F, Nicoud J F, Nierengarten J-F, Liu S G, Barigelletti F, Armaroli N, Ouali L, Krasnikov V and Hadziioannou G 2000 *J. Am. Chem. Soc.* **122** 7467
[176] Schmidt-Mende L, Fechtenkötter A, Müllen K, Moons E, Friend R H and MacKenzie J D 2001 *Science* **293** 1119